We are IntechOpen, the world's leading publisher of Open Access books Built by scientists, for scientists

6,900
Open access books available

186,000
International authors and editors

200M
Downloads

Our authors are among the

154
Countries delivered to

TOP 1%
most cited scientists

12.2%
Contributors from top 500 universities

WEB OF SCIENCE™

Selection of our books indexed in the Book Citation Index in Web of Science™ Core Collection (BKCI)

Interested in publishing with us?
Contact book.department@intechopen.com

Numbers displayed above are based on latest data collected.
For more information visit www.intechopen.com

11

Study on Thixotropic Plastic Forming of Magnesium Matrix Composites

Hong Yan
Department of Materials Processing Engineering, Nanchang University, China

1. Introduction

Magnesium alloys have a lot of advantages in mechanical and physical properties such as lightness, high specific strength, good thermal conductivity and damping. They are widely developed for automobile, spaceflight, electron, light instrument and so on. The damping capacity of materials plays a critical role in regulating the vibration of structure, decreasing the noise pollution and improving the fatigue properties of workpiece under circulating loading. Magnesium and its alloy have higher thermodynamically stability and aging stability as well as better damping capacity, whose applications are limited because of their poor mechanical properties. Creep is an important characteristic of mechanics behavior of metal at high temperature, which is a phenomenon for plastic deformation taken place slowly on the condition of constant temperature of long time and constant load. For the industrial application fields such as automobile industry and aviation industry, the creep is an important index to measure the good or bad property of a material at high temperature. The strength and creep resistance of magnesium alloys (AZ91D and AM60 alloys) are rapid decreased when the temperature is beyond 150℃. There are the disadvantages such as poor strength and toughness and poor creep resistance in magnesium alloy applied process, which limits its farther application. So it is an important to develop the magnesium matrix composites (MMCs) of high strength and toughness and good creep resistance and its forming technology. Specially, particle-reinforced magnesium matrix composites are characterized by low cost and simple process, which is a research focus of MMCs fields [Hai et al., 2004]. However, magnesium possesses low melting point, high chemical activity and ease of flammability, so preparing magnesium matrix composites is difficult in some extent. As a result, it is important to seek a better fabrication method for magnesium matrix composites [Zhou et al., 1997]. Powder metallurgy (PM) and casting are common methods for obtaining these composite materials. PM process needs complex equipments with higher expense, and can't fabricate large sized and complicated MMCs components. It has hazards such as powder burning and exploding. In contrast, casting method can produce large sized composites (up to 500kg) in industry at mass production levels with its simple process and convenient operation because of few investing equipment and low cost. So MMCs fabricated by casting process are now investigated by many researchers [Kang et al., 1999].

The plastic formability of MMCs is poor, which need to introduce an advanced forming method. With the growing development of semi-solid forming technology, the thixoforming

technology of magnesium matrix composites is a new method. The semi-solid material forming technology has advantages such as lower deformation resistance, good material mobility and so on [Flemings 1991, Yan et al., 2005]. It was composed of three processes such as: semi-solid billet fabrication [Yan et al., 2005], partial remelting [Yan et al., 2006] and thixoforming [Yan et al., 2008]. For this reason, the research on the basic theory of semi-solid stirring melting fabrication method and thixoforming process for the advanced MMCs is studied in this item. The works include the study of semi-solid stirring melting fabrication method [Yan & Fu et al., 2007; Yan & Lin et al., 2008] and reheating process [Yan & Zhang et al., 2008; Zhang et al., 2011] for the particle-reinforced MMCs. The material constitutive relation will be proposed [Yan & Wang et al., 2011]. Then the finite element model coupled with multi-physical fields will be built. The simulation will be gone based on the developed analytical program. The forming performances and deformed laws in the thixoforming for the particle-reinforced MMCs will be studied by the way of combining theoretical analysis with experimental method [Yan & Huang, 2011]. The results will play an important function to bulid the theoretical and technological fundament for the thixoforming process of the particle-reinforced MMCs applied the industry area.

2. Study on fabrication methods and various properties for magnesium matrix composites

2.1 Fabrication methods

The AZ61 alloy was used as the matrix material. The chemical composition of AZ61 was 5.8%～7.2%Al, 0.15% Mn, 0.40%～1.5%Zn, 0.10% Si, 0.05%Cu, 0.05%Ni, 0.005%Fe, and the rest is Mg. Its solidus temperature was 525℃, and the liquidus temperature was 625℃. The reinforcement was green α-SiC particle whose average diameter was $10_{\mu m}$. A self-manufactured electric resistance furnace was used for melting Mg alloy (shown in Fig.1). The liquid metal was stirred with the mechanical stirrer driven by the timing electrical machine in the melting process. In order to improve the accuracy of controlling temperature, the thermocouple was inserted directly into the liquid metal, and combined with the artificial aptitude modulator BT608 that adopted the industrial micro-processor, whose precision was only ±10℃. The MMCs specimens were sampled by the pipette connecting to a vacuum pump in this experiment.

The fabrication processes of SiCp/AZ61 composites were described as follow. AZ61 alloy matrix was heated to melt, gas was gotten rid of and slag was removed. Then SiC reinforcement was added into the molten. There were the three addition processes. In the fully-liquid stirring casting process (about 680℃), SiC particles were introduced into the fully-liquid molten, and then sampled after stirred to reach predetermined time. (2) In the stirring-melt casting process (590℃), SiC particles were introduced at the semi-solid state, then sampled after reached to a fully-liquid temperature of 680℃. (3) In semi-solid stirring casting process, SiC particles were introduced at the semi-solid state, then sampled after stirred to reach predetermined time. In above experiments, their volume fractions of SiC particles were 3%, 6%, and 9% respectively, whose preheated temperature was 500℃ with holding time 2h. The stirring rate was 500r/min with holding time 10min. Then the specimen was made to the metallurgical phase sample and corrupted with 0.5% ammonium HF liquor, and its microstructural changes were observed under the optical microscope. Finally, the Vickers hardness was measured in a micro-sclerometer HXS-1000AK.

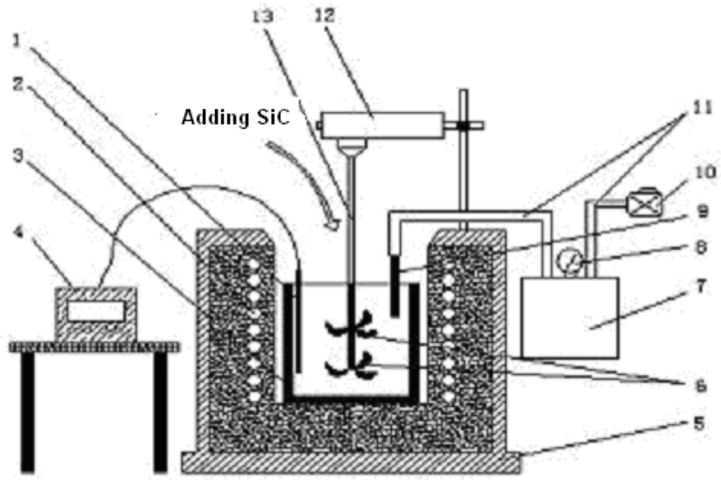

Fig. 1. Schematic diagram of SiCp/AZ61 composites fabricated in stirring casting process 1. thermocouple 2. resistance thread 3. crucible 4. BT608 (artificial aptitude modulator) 5. resistance furnace 6. strring lamina 7. vacuum jar 8. pressure meter 9. pipette 10. vacuum pump 11. guiding windpipe 12. timing electrical machine 13. stirring bar

The microstructures of SiCp/AZ61 composites in three casting processes were shown in Fig.2. The variations of influence of three casting processes on the microstructures of SiCp/AZ61 composites were shown in Fig.2- Fig.4. The distribution of SiC particles was a little uniform in the fully-liquid casting process where a lot of gas cavities and slacks were presented, and SiC particles were easy to sink and float. There were a few gas cavities in the semi-solid casting process where the distribution of SiC particles was inhomogeneous. SiCp/AZ61 composites fabricated by the stirring-melt casting method possessed not only few gas cavities but fairly uniform distribution.

The existence of gas cavities and slacks was attributed to the following factors: (1) Gas was involved in the molten during the mechanical stirring process. (2) Their non-uniform volume shrinkages presented in the composites solidification process due to the differences of their thermal expansion coefficient and heat conduction between matrix and reinforcement. (3) Hydrogen produced in the chemical reactions between Mg and H_2O was dissolved in the molten and formed gas cavities during solidification. (4) The formation of gas cavities was resulted from the particles clustering.

The main problem in the stirring casting process was the inhomogeneous distribution of reinforcement phase. The major reasons were followed as. (1) Due to having the different densities between matrix and reinforcement, SiC particles were settled down. (2) The higher surface tension and poor wettability between SiC and matrix presented, a few SiC particles were floated on the surface of the molten.

SiC particles were introduced at the semi-solid state during the semi-solid stirring casting process where the high viscosity semi-solid alloy can help withstand SiC particles from sinking and floating, but the uniform distribution can not be solved (shown in Fig.3). During the stirring-melt casting process the reinforcement were added at the semi-solid state, and the composites were poured immediately after reached 690℃ (liquidus). The quite uniform SiCp/AZ61 composites can be obtained in this method (shown in Fig.4).

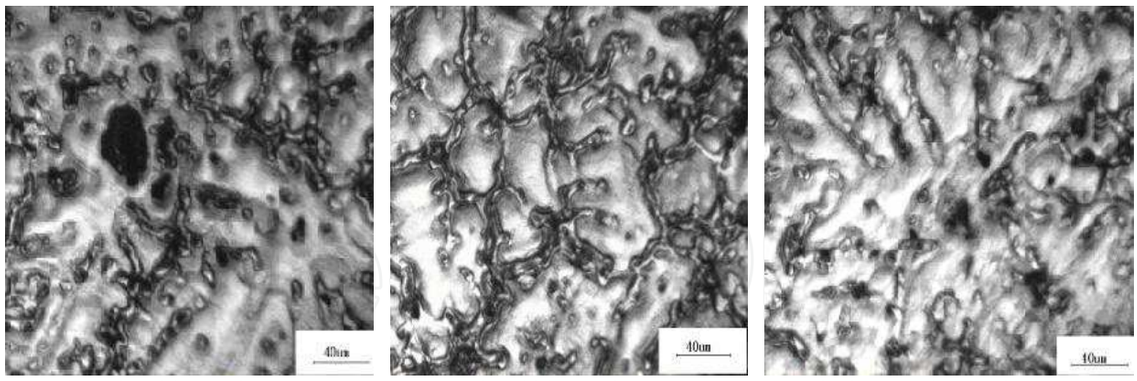

(a) fully-liquid casting process (b) semi-solid casting process (c) stirring-melt casting process

Fig. 2. Microstructures of SiCp/AZ61 composites in three casting processes

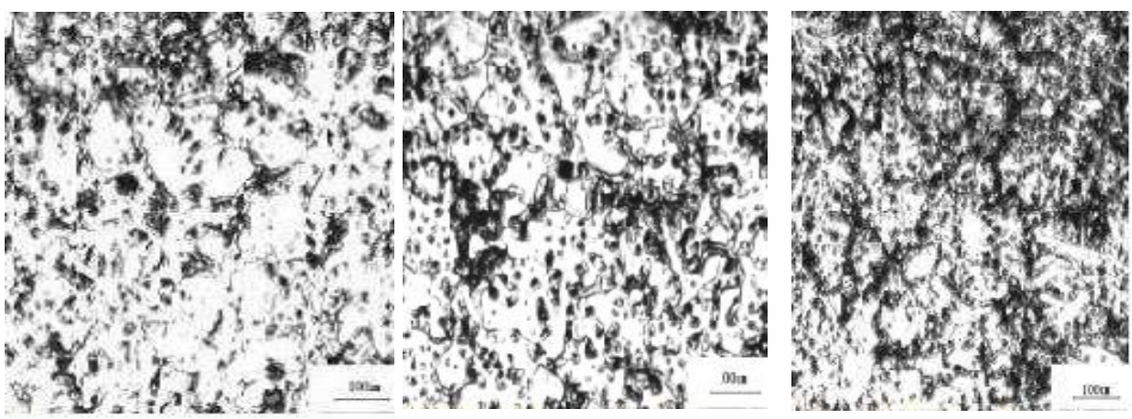

(a) 500r/min, 10min, 3Vol.% (b) 500r/min, 10min, 6Vol.% (c) 500r/min, 10min, 9Vol.%

Fig. 3. Microstructures of SiCp/AZ61 composites with various volume fractions of SiC particles in semi-solid stirring casting process

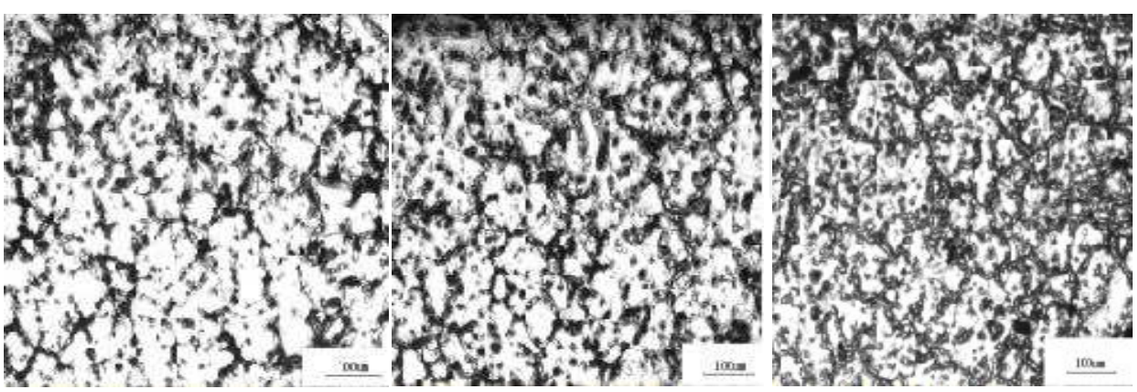

(a) 500r/min, 10min, 3Vol.% (b) 500r/min, 10min, 6Vol.% (c) 500r/min, 10min, 9Vol.%

Fig. 4. Microstructures of SiCp/AZ61 composites with various volume fractions of SiC particles in stirring-melt casting process

2.2 Optimization on stirring melt casting process

In this study, the composites were fabricated by a stirring melt casting method. The effects of volume fraction of SiC particles, stirring temperature and stirring time on the mechanical properties and microstructure of SiCp/AZ61 composites were investigated. The main technological parameters of preparing SiCp/AZ61 composites were optimized, which was helpful for obtaining its good properties.

The effects of volume fraction of SiC particles, stirring temperature and stirring time on the mechanical properties of SiCp/AZ61 composites were investigated by an orthogonal experimental method, in which average particle size and stirring speed were maintained the same. The orthogonal test table with three factors and three levers is shown in Table 1. According to design of the primary experiment, volume fractions of SiC particles were 3%, 6% and 9%, stirring temperatures were 580℃, 587℃ and 595℃, and stirring times were 3min, 5min and 7min. Three factors were volume fraction of SiC particles, stirring temperature and stirring time. Two targets were tensile strength and elongation.

level	volume fraction of SiC A (*%)	stirring temperature B (^{0}C)	stirring time C (min)
1	3	580	3
2	6	587	5
3	9	595	7

Table 1. Factors and levels of test

The effects of volume fraction of SiC particles, stirring temperature and stirring time on the tensile strength and elongation at room temperature of SiCp/AZ61 composites are shown in Table 2. (1) Tensile Strength Analysis. The level two (the volume fraction of SiC 6%) was

No.	volume fraction of SiC A	stirring temperature B	stirring time C	tensile strength /MPa	elongation /%
1	1	1	1	172	3.8
2	1	2	2	179	4.2
3	1	3	3	163	5.2
4	2	1	2	184	3.5
5	2	2	3	176	4.1
6	2	3	1	189	3.9
7	3	1	3	164	1.3
8	3	2	1	153	1.9
9	3	3	2	170	2.1
I	171.3	173.3	171.3		
II	183.0	169.3	177.7		
III	162.3	174.0	167.7		
R (tensile strength)	20.7	4.7	10.0		
I	4.4	2.9	3.2		
II	3.8	3.4	2.1		
III	1.7	3.7	3.5		
R (elongation)	2.7	0.8	1.4		

Table 2. The table of three factors and three levels in the orthogonal experiment

the best among the levels of factor A. The level three (595℃) was the best among the levels of factor B. The level 2 (5 min) was the best among the levels of factor C. Thus the optimum combination was $A_2B_3C_2$. (2) Elongation analysis. The level two (the volume fraction of SiC 3%) was the best among the levels of factor A. The level 3 (595℃) was the best among the levels of factor B. The level three (7 min) was the best among the levels of factor C. Thus the optimum combination was $A_1B_3C_3$. (3) Range Comprehensive Analysis. The greater the Range (R), the greater the effect of the lever change of the factor on the test target. This factor was more important. From Table 2, the sequence of tensile strength was $R_A>R_C>R_B$. So the sequence of primary and secondary in factors of A, B, C was the volume fraction of SiC particles, stirring time and stirring temperature. The sequence of elongation was $R_A>R_C>R_B$. So the sequence of primary and secondary in factor of A, B, C was also the volume fraction of SiC particles, stirring time and stirring temperature. Besides, from the ranges(R) in table 1, factor A has a more notable impact for tensile strength and elongation, and other factors do not have great impact. After comprehensive analysis, a better combination of factors was $A_2B_3C_2$, namely, the optimum processing plan of SiCp/AZ61 composites in the experimental condition was volume fraction of SiC particles 6%, stirring temperature 595℃ and stirring time 5 min.

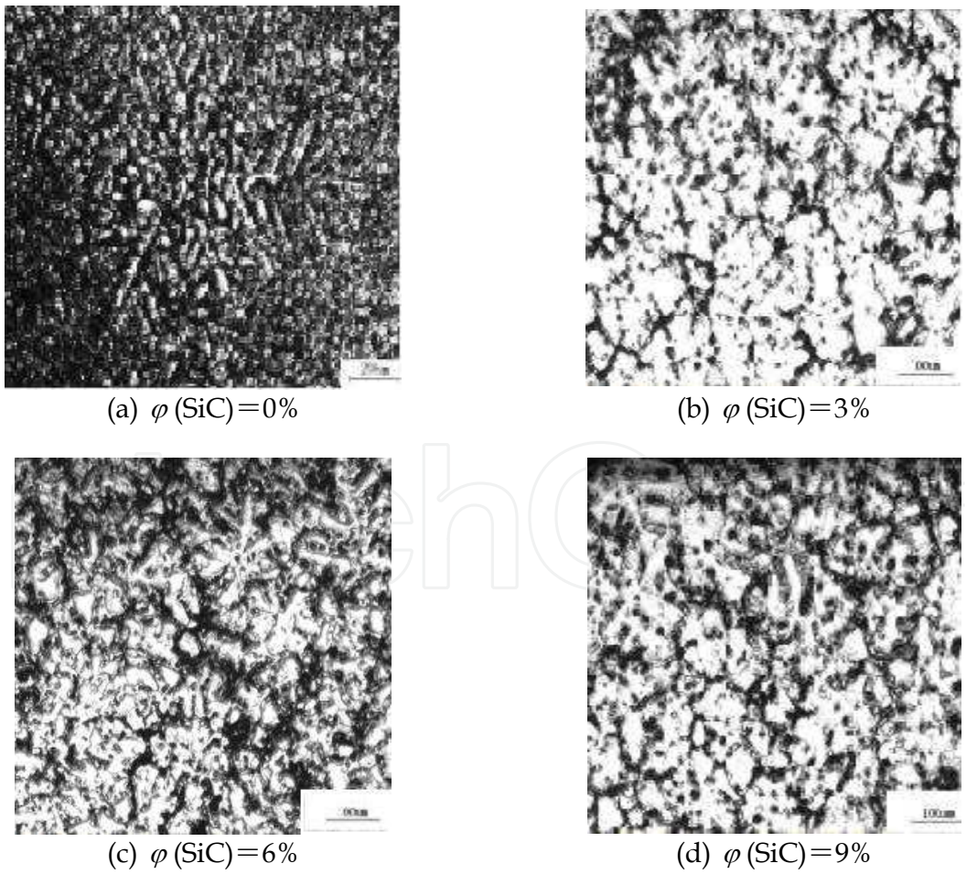

(a) φ(SiC)=0% (b) φ(SiC)=3%

(c) φ(SiC)=6% (d) φ(SiC)=9%

Fig. 5. Microstructures of SiCp/AZ61 composites with various volume fractions of SiC particles

The test results showed that the tensile strength of SiCp/AZ61 composites, that increased as the increasing of volume fraction of SiC particles increasing, and were higher than that of AZ61 (about 165MPa). The tensile strength was up to the maximum 189MPa when the volume fraction of SiC particles was 6%. However, the tensile strength decreased as the volume fraction of SiC particles increased continuously. Comparison with the volume fractions of SiC particles, the change trend of elongation decreased gradually with addition of SiC particles. The reason was a mass of rigid second phase existence in the matrix of SiCp/AZ61 composites, which could improve its rigidity and tensile strength. With the increasing volume fraction of SiC particles, problems of particle packing, agglomerating and clustering were presented in the matrix (Fig. 5), which caused tensile strength to decrease. Decreasing elongation was due to the non-uniform distribution of SiC particles and weak cracks in boundaries between the reinforcement and matrix.

The fracture morphology of AZ61 matrix at the ambient temperature is shown in Fig.6a. Ductility dimples existed, and cleavage cracks were present in a part. Fig.6b showed the fracture morphology of SiCp/AZ61 composites at the ambient temperature by a better processing plan ($A_2B_3C_2$). Compared with the fracture morphology of the matrix, the fracture morphology of SiCp/AZ61 composites at the ambient temperature were brittle where the fractured SiCp particles were found (Fig. 7a).

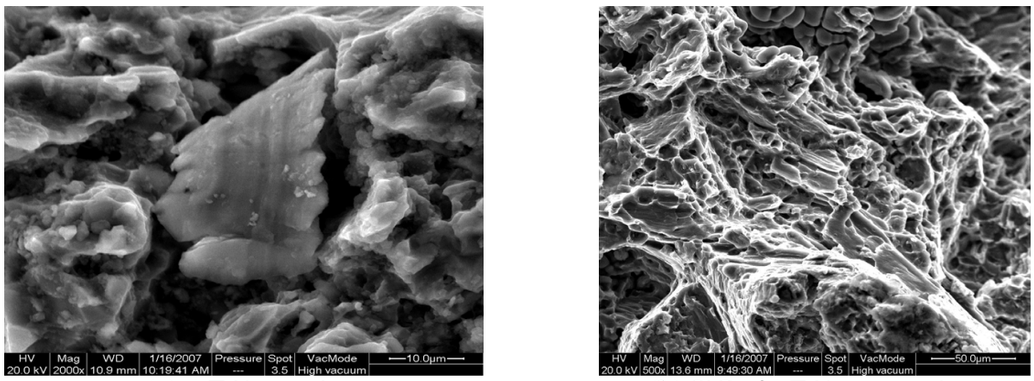

(a) AZ61 matrix (b) SiCp/AZ61 composites

Fig. 6. SEM of tensile fracture surfaces

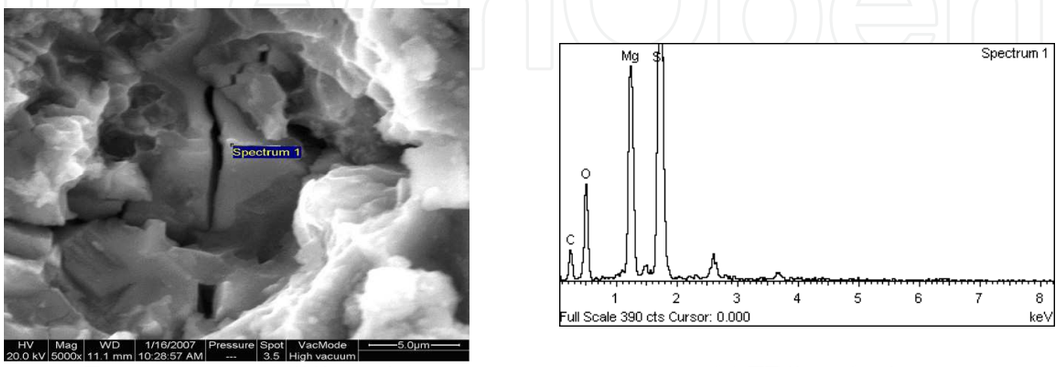

(a) Fractographs of SiC particle (b) EDS analysis

Fig. 7. Fractographs of SiC particle and EDS analysis

3. Semi-solid isothermal heat treatment technology for the partial remelting of composites

In this study, semi-solid isothermal heat treatment technology was used for the partial remelting of composites. The round semi-solid microstructure had been obtained by controlling the reheating processing parameters such as heating temperature and isothermal holding time. The law of microstructural evolution in the remelting process of SiCp/AZ61 composites was investigated, which was expected to offer some theoretical references for the design of thixoforming technology.

The reheating temperatures were taken as 590℃, 595℃, 600℃ and 610℃ respectively with isothermal temperature heat treatment times of 15min, 30min and 60min. When the scheduled time and temperature were reached, the specimen was taken out and water quenched. Then the specimens were made and etched with 4% nitic acid liquor, and its microstructure change was observed under the optical microscope. The Image-pro Plus software was used to measure the diameter of equal-area of microstructure. The average radius of grain microstructure was then calculated.

According to the Sheil equation (1) and equation (2), the liquid phase volume fraction of the partial remelting structure was calculated (shown in Fig.8).

$$f_L = \left(\frac{T_m - T}{T_m - T_L} \right)^{-1/1-K_0} \tag{1}$$

$$f_E = f_S(1 - f_P) - f_P \tag{2}$$

Where f_L , f_E and f_P represent the liquid phase volume fraction of matrix alloy, effective liquid phase volume fractions of composites and enforcing particles. T_m and T_L are melting point of the pure metal and the liquidus temperature of the alloy. K_0 is represented for the coefficient of distribution.

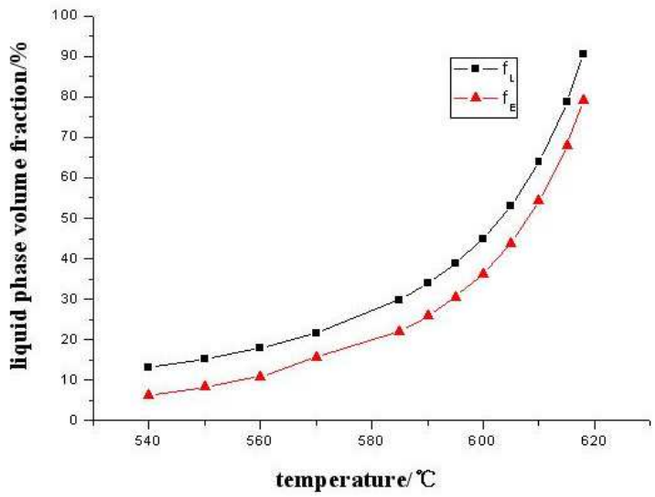

Fig. 8. Relationship between liquidphase volume fraction and temperature

Fig. 9. shows the microstructural evolution of SiCp/AZ61 composites during partial remelting. When the heating temperature reached 590℃ with isothermal holding time of 15min, the grain boundaries had almostly been merged and could not be seen clearly. At the same time, SiC particles were inside the grains away from the grain boundaries (Fig. 9a). A separating tendency in the grains of coalescence emerged with the prolongation of isothermal holding time (Fig. 9b). While the holding time reached 60 min, a few grain boundaries became clear. A few globular grains appeared with SiC particles presented in the grain boundaries, but the liquid volume fraction was lower (Fig.9c). When the reheating temperature increased to about 595℃ with holding time of 15 min, the grain microstructure evolved quickly, and a globular microstructure appeared, then the eutectic structure began to melt (Fig.9d). The grain boundaries appeared completely with holding time 30 min, and fine globular grains emerged. The effective liquid fraction of SiCp/AZ61 composites was about 31%, and the mean diameter of grains was approximately 60μm (Fig.9e). When the isothermal holding time was further increased to 60min, the grain microstructure was entirely spheroidized, which became more clear and round, and SiC particulate returned to the grain boundaries from interior of grains (Fig.9a,b). At the same time, the mean diameter of grains was about 85μm (Fig.9f). As the reheating temperature increased to 600℃ with holding time of 15 min, the microstructural evolution of the sample during remelting was rapid. Some of grains began to spheroidize (Fig.9g). When the holding time reached 30 min, all grains had been spheroidized, whose sizes became relatively fine (Fig.9h). With the prolongation of holding time to 60 min, the grain microstructure tended to spheroidize and increase in size, and the effective liquid fraction was about 37% (Fig.9i). When the reheating temperature was above 610℃, the semi-solid microstructure began to dissolve and disappear. The specimens were susceptible to serious deformation, the liquid flow emerged from the sample, which would prevent semi-solid microstructure from partial remelting (Fig.9j). Therefore the optimal technological parameters of SiCp/AZ61 composites were the reheating temperature of 595℃～600℃ and isothermal holding time of 30min～60min.This temperature interval was suitable for semi-solid thixoforming of SiCp/AZ61 magnesium matrix composites.

The microstructures of SiCp/AZ61 composites during partial remelting (Fig.9e, f) were compared with that of AZ61 alloy (Fig.10). It was observed that the microstructures of SiCp/AZ61 composites coalescenced basically before isothermal holding time at the predetermined temperature for 15min, and a separating tendency in the grains didn't appear obviously. After isothermal holding at the predetermined temperature for 25min, the grain microstructure began separating and spheroidizing. However the rate of separation and spheroidization for AZ61 alloy increased. When the reheating temperature reached 595℃ with holding time of 0min,the grain microstructure was separated completely, and a few globular grains had appeared. With the prolongation of holding time from 20min to 40min, the mean diameter of the globules was 85μm and 110μm respectively. In addition, compared with AZ61 alloy, the microstructures of SiCp/AZ61 composites were finer during partial remelting due to addition of SiC particulates. Coalescence was restricted since the globules were isolated one with respect to the other by the presence of SiC particulates. At the same time the effective diffusion coefficient of the liquid phase was also reduced because of the presence of reinforced particulates, and during the subsequent isothermal holding process coalescence of α phase was hindered, and Ostwald ripening was also restricted.

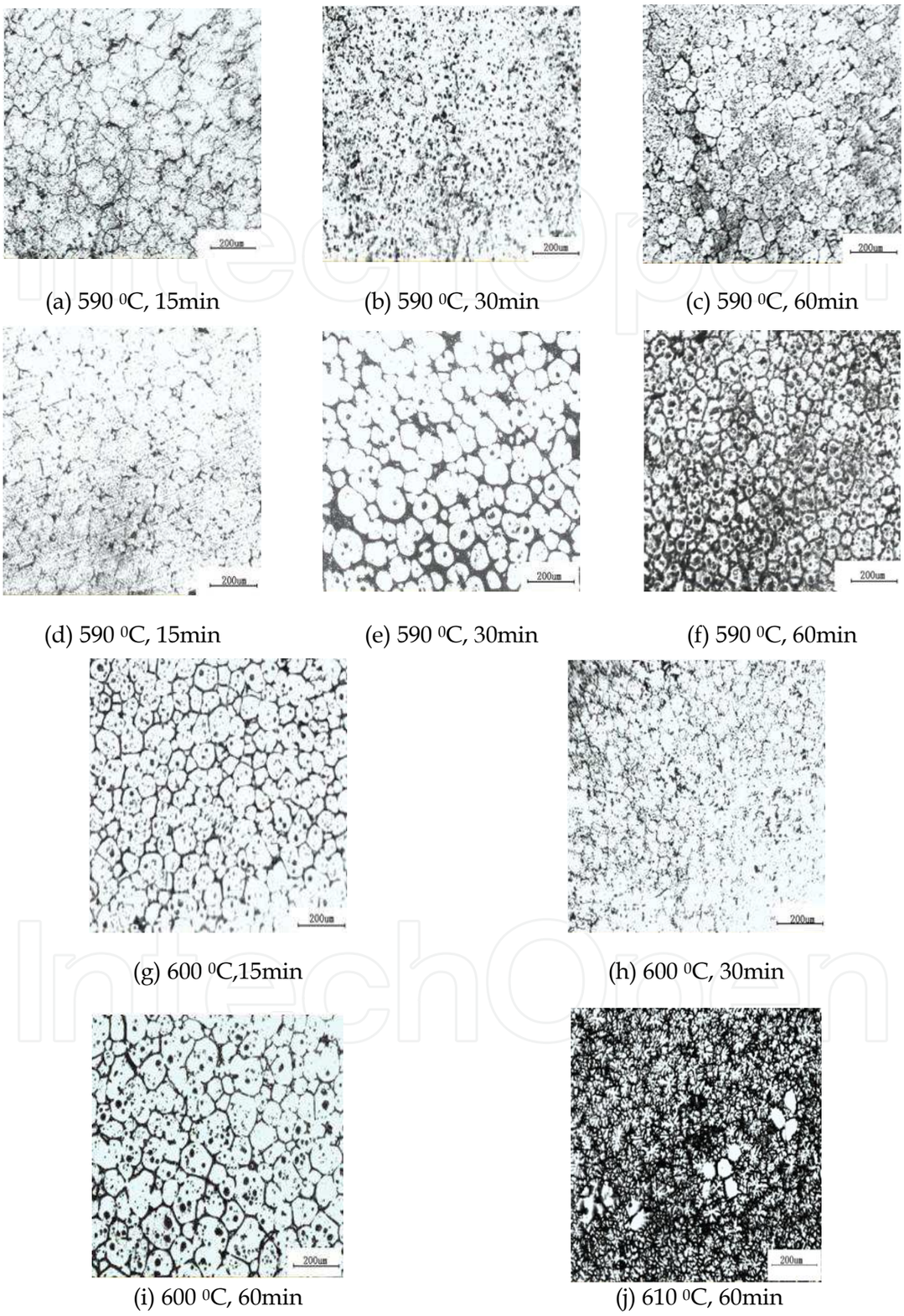

(a) 590 ^{0}C, 15min (b) 590 ^{0}C, 30min (c) 590 ^{0}C, 60min

(d) 590 ^{0}C, 15min (e) 590 ^{0}C, 30min (f) 590 ^{0}C, 60min

(g) 600 ^{0}C,15min (h) 600 ^{0}C, 30min

(i) 600 ^{0}C, 60min (j) 610 ^{0}C, 60min

Fig. 9. The microstructural evolution of SiCp/AZ61 composites during partial remelting

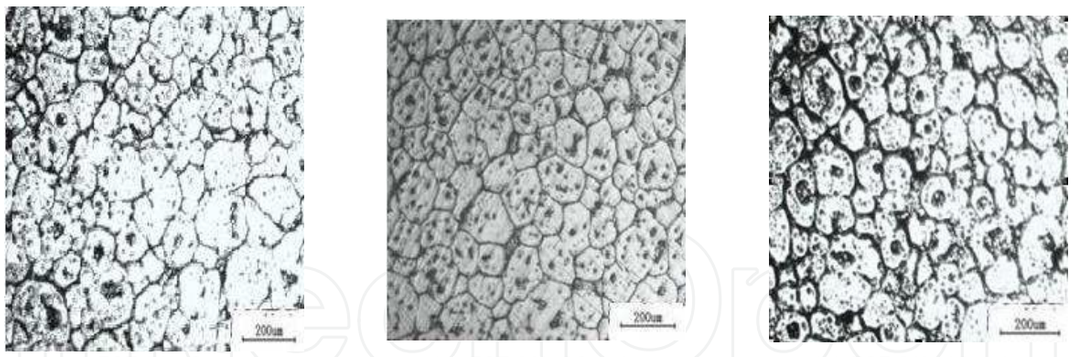

(a) 595 ^{0}C, 0min (b) 595 ^{0}C, 20 min (c) 595 ^{0}C, 40 min

Fig. 10. Microstructures of semi-solid AZ61 magnesium alloy billet during partial remelting

4. Thixotropic compression deformation behavior of composites

The characteristics of semi-solid composites deformed mechanism can be understood well only when the relationships between stress and strain are described. So the semi-solid compression tests for SiCp/AZ61 composites were conducted, whose mechanical properties and destruction model were investigated.

The experiments were conducted in a Thermecmastor-Z dynamic material testing machine, whose set-up was shown in Fig.11. The specimen was heated by electromagnetic wave, whose temperature was monitored by thermocouples. The graphite slices were placed between the specimen and the compression heads for reducing the influence of friction on experiment. In order to study and master the characteristic mechanics of semi-solid magnesium matrix composites at high solid volume fractions, the deformation temperatures were taken as 530℃, 545℃, 560℃ and 570℃ respectively. According to the heating procedure shown in Fig.12, the initial heating rate was 10℃/s; when the specimen temperature reached 500℃, the temperature rate was down to 1℃/s. Then the semi-solid compression experiments were done under the strain rates of 0.1s^{-1}, 0.5 s^{-1}, 5.0 s^{-1}and 10 s^{-1} respectively, in which the total strain was 0.6.

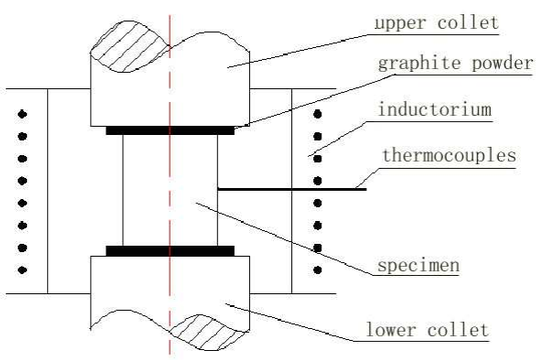

Fig. 11. Schematic diagram for the compressive tests

The stress-strain curves of semi-solid SiCp/AZ61 composites with various volume fractions of SiC particles are shown in Fig.13. The tendency of curves implies that the deformation temperature has a significant effect on the flow stress. It is observed that for a constant strain

rate and constant volume fraction of SiC in the composites, the flow stresses and peak stresses decrease with the increasing of deformation temperature, which presents that the thixotropic plastic deformation of the composites is highly sensitive to temperature. The tendency is thought to be the result of variation of volume fractions of solid α phase. When the specimens has high solid volume fractions, the solid grains contact with each other and form a net, sliding and rotation of grains become hard. The plastic deformation of solid particles is the main mechanisms. With the increasing of temperature, the solid volume fractions decrease, and the solid grains are surrounded by liquid phase, which makes the solid grains to slid and rotate easily. Thus the sliding and rotation of grains plays a more significant role in the thixotropic plastic deformation.

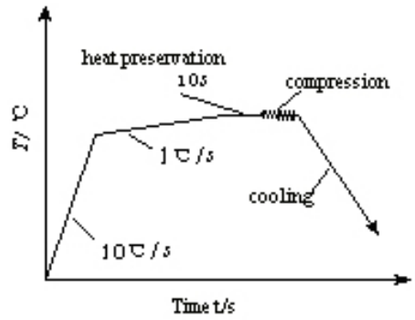

Fig. 12. Heating processing

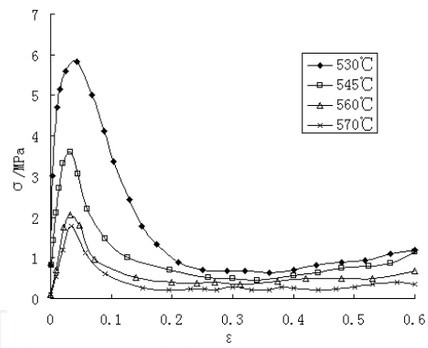

(a) f_p=3%, $\dot{\varepsilon}$ =0.1 s^{-1}

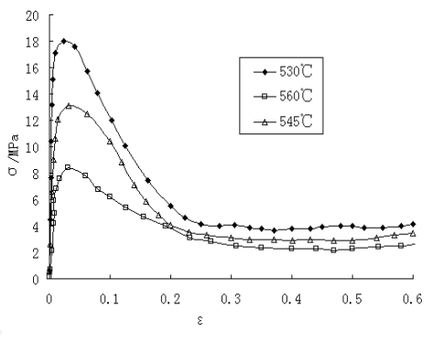

(b) f_p=6%, $\dot{\varepsilon}$ =5s^{-1}

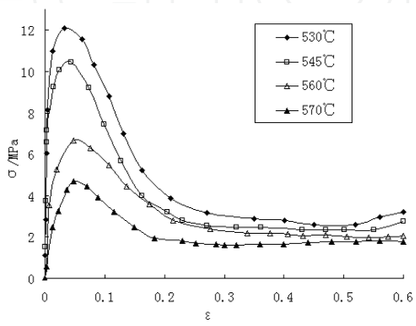

(c) f_p=9%, $\dot{\varepsilon}$ =10s^{-1}

Fig. 13. Curves of stress-strain relation at various temperatures for SiCp/AZ61 composites

Relationships between peak stress and temperature of composites with strain rate of $10s^{-1}$ are shown in Fig.14. It can also be seen that the variation of volume fractions of SiC has a significant effect on the peak stress of the composites. When the deformation temperature raises slightly higher than the solid phase line in semi-solid zone, the volume fractions of liquid phase is low in the matrix, and the peak stress decreases rapidly almost as linear form with the increasing of temperature initially, and then slows as the temperature increases further. The results are thought to be of the lower volume fractions of liquid phase. When the specimens has high volume fractions of solid phase , the solid grains contact with each other to form a net, the sliding and rotation of grains become hard. The plastic deformation of solid particles is the main mechanisms. Besides SiC particles increase the resistance to grain boundaries sliding and impose barriers to dislocation motion, which leads to higher resistance for plastic deformation. With the increasing of temperature, the volume fractions of liquid phase increase, and the solid grains are surrounded by liquid phase, which requires smaller force for the solid grains to slid and rotate. Thus the peak flow stress decrease rapidly, and then slowed as the temperature increases further.

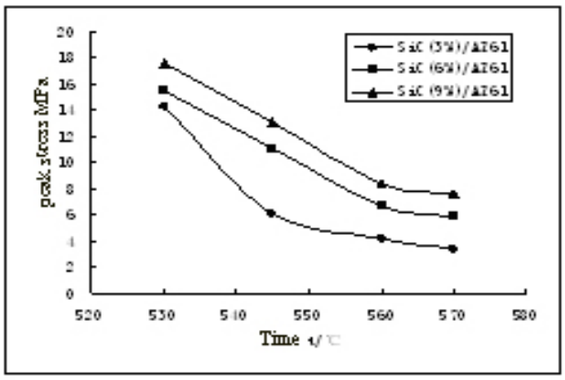

Fig. 14. Relationships between the peak stress and temperature of three SiCp/AZ61composites in semi-solid thixotropic compression

The relations of stress-strain rate at various strain rates are shown in Fig. 15. It can be seen that the peak stress increases as the strain rate increases at the constant temperature. When the composites are compressed at high strain rate (for example 10 s^{-1}), the liquid phase can not be squeezed out timely, in which the flow stress is very high during the initial deformation stage, and then decreases as the result of high shearing rate. With the further deformation, the liquid is squeezed out and pushed together, in which the solid particles are smashed. During this stage, the grain boundaries sliding and flow become easy and the flow stress decreases rapidly. At lower strain rate the solid grains are surrounded by liquid phase, which requires smaller force for sliding and rotation. So the flow stress is lower.

Fig. 16 presents stress-strain curves of the SiCp/AZ61 composite with different SiC fractions at 545℃and 560℃ and constant strain rate of $0.1s^{-1}$ and $10s^{-1}$. The fractions of SiC have a significant effect on the flow stress. The compression stress increases with the increasing of volume fractions of SiC particles. The reason is that SiC particles are mainly located in the inter-granular and boundary regions in the composites. The SiC particles impose barriers to dislocation motion and resistance to the solid grains sliding during the steady-state compressive deformation. So it increases the resistance for dislocation and grain boundaries sliding with the increasing of volume fractions of SiC particles.

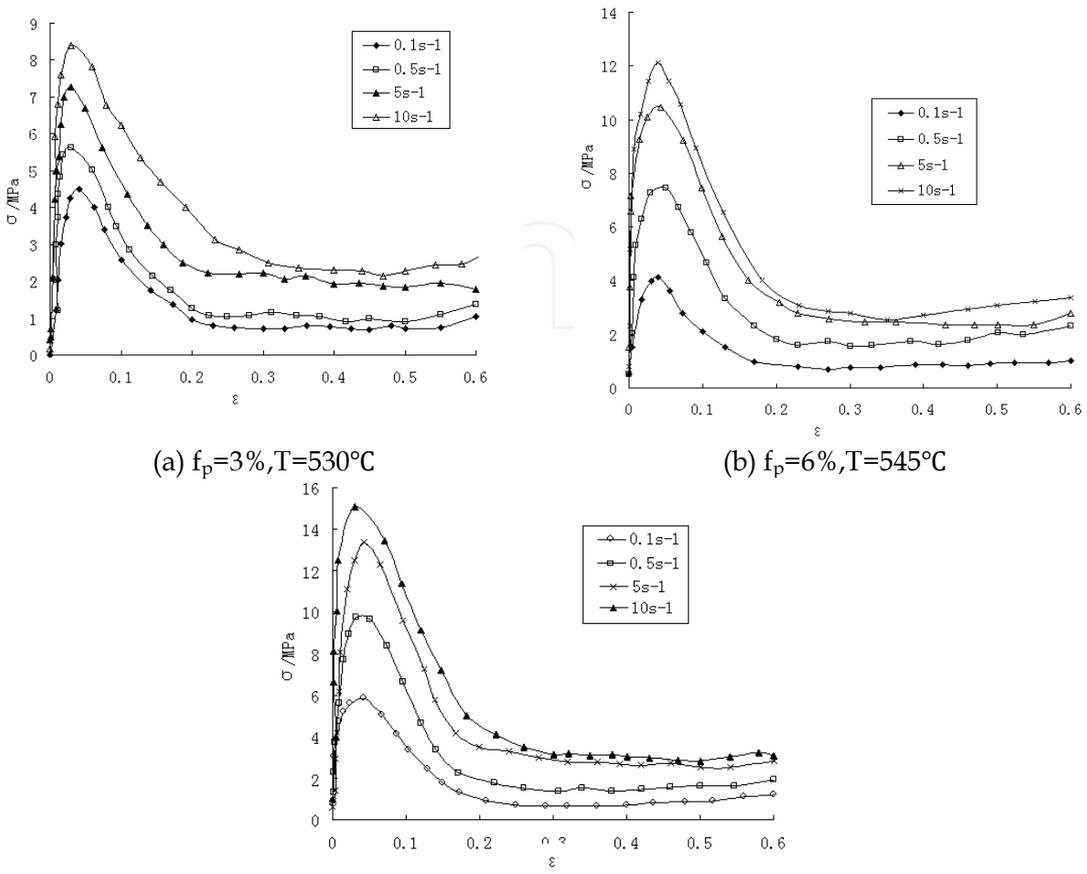

(a) f_p=3%,T=530℃ (b) f_p=6%,T=545℃

(c) f_p=9%,T=570℃

Fig. 15. Curves of stress-strain relations at various strain rates for SiCp/AZ61 composites

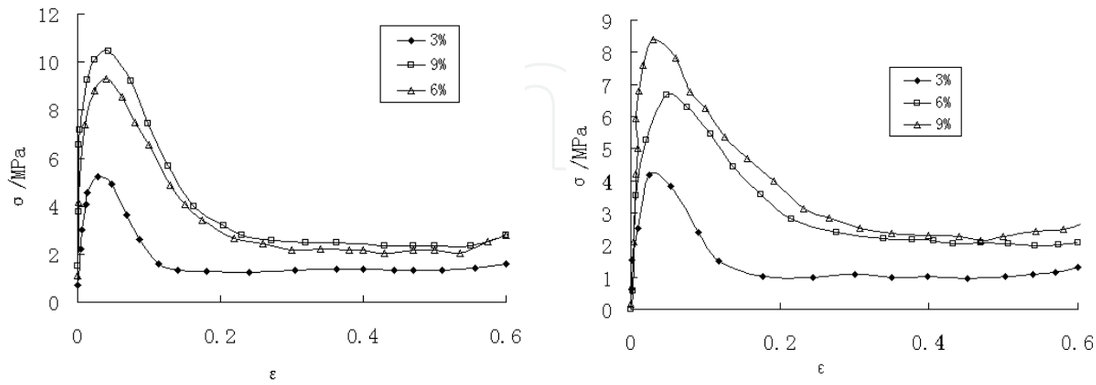

(a) T=545℃, $\dot{\varepsilon}$ =0.1s^{-1} (b) T=560℃, $\dot{\varepsilon}$ =10s^{-1}

Fig. 16. Curves of stress-strain relation at 545℃and 560℃ for SiCp/AZ61 composites with different SiC fractions

The appearances of specimens compressed at semi-solid state are shown in Fig. 17. In can be seen that the surface longitudinal cracks of specimen happen at compression ratio of 20% and the liquid phase is squeezed out along the cracks. When the compression ratio reaches up 30%, the volume fractions of liquid phase squeezed out of the surface increases, which generates the mixed liquid-solid outer surfaces. The surface strength is very low and generates easily cracks. When all of liquid is squeezed out, the flow stress starts to ascend. At last the compressed specimen looks like popcorn.

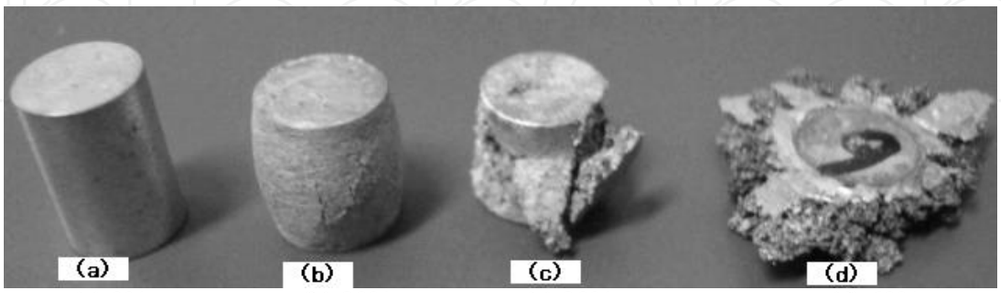

(a) 0% (b) 20% (c) 30% (d) 60%

Fig. 17. Appearances of specimens compressed at semi-solid state

5. Constitutive model for thixotropic plastic forming of composites

On the basis of analysis of behavior of thixotropic plastic deformation of composites in compression process, its constitutive model is established. Then the model parameters are determined using the multiple nonlinear regression method.

Based on the experimental analysis of axial compression of composites in semi-solid state, there is a certain non-liner relationship among stress σ and strain rate $\dot{\varepsilon}_z$, strain ε_z, temperature T, liquid phase rate f_L, as well as the volume fraction of reinforcement f_p [Yan & Wang, 2011]. At the same time Hong Yan present the constitutive relationship of semi-solid magnesium alloy as follow [Yan & Zhou, 2006]:

$$\sigma \propto \exp(1/T)\dot{\varepsilon}^{a_1}\varepsilon^{a_2}(1-\beta f_L)^{a_3} \tag{3}$$

Where σ – stress, ε – strain, $\dot{\varepsilon}$ – strain rate, T – temperature, β – geometric parameters(β＝1.5), f_L – liquid phase rate.

In the study of deformation behavior of composites under high strain rate [Bao & Lin, 1996] and [Li & Ramesh, 2000] found that the influence of volume fraction of reinforcement on the mechanical behavior of the material was present as following:

$$\sigma(f_p) = \sigma(\varepsilon,\dot{\varepsilon})\cdot g(f_p)\cdot[1+(\alpha\dot{\varepsilon})^m f_p] \tag{4}$$

Where σ- stress, ε- strain, $\dot{\varepsilon}$ - strain rate, $\sigma(\varepsilon,\dot{\varepsilon})$ - function of strain and strain rate, fp- volume fraction of reinforcement.

So the constitutive model of thixotropic plastic deformation of composites reinforced with particles is proposed.

$$\sigma = \exp(d/T)\cdot\varepsilon^{n}\cdot\dot{\varepsilon}^{m}\cdot[1-\beta f_L]^{a_1}\cdot g(f_p)\cdot[1+(\alpha\dot{\varepsilon})^{m} f_p]^{a_2} \tag{5}$$

Under assumption of $g(f_p) = e^{a+bf_p+cf_p^{\,2}}$ the constitutive model is established in the following form.

$$\sigma = \exp(a+bf_p+cf_p^{\,2}+d/T)\cdot\varepsilon^{n}\cdot\dot{\varepsilon}^{m}\cdot[1-\beta f_L]^{a_1}\cdot[1+(\alpha\dot{\varepsilon})^{m} f_p]^{a_2} \tag{6}$$

Where a, b, c, d, a_1, a_2 - constant, n—strain hardening index, m—strain rate sensitivity index,β—constant (β=1.5), α - correction coefficient , fp - volume fraction of reinforcement, f_L - liquid phase rate. $f_L = (\frac{T_M - T_L}{T_M - T})^{\frac{1}{1-K}}$, T_M - the melting point of pure metal, T_L - liquidus temperature of alloy, k - balance coefficient.

The parameters in proposed constitutive model were determined by the multiple nonlinear regression method. The nonlinear equation is transformed into linear one using legarithms for Esq.(3).

$$\ln\sigma = a+bf_p+cf_p^{\,2}+d/T+n\ln\varepsilon+m\ln\dot{\varepsilon}+a_1\ln(1-\beta f_L)+a_2\ln[1+(\alpha\dot{\varepsilon})^{m} f_p] \tag{7}$$

Where

$$\begin{aligned} &y=\ln\sigma, X_1=f_p, X_2=f_p^{\,2}, X_3=1/T, X_4=\ln\varepsilon, X_5=\ln\dot{\varepsilon}, X_6=\ln(1-\beta f_L),\\ &X_7=\ln[1+(\alpha\dot{\varepsilon})^{m} f_p]\\ &A_0=a, A_1=b, A_2=c, A_3=d, A_4=n, A_5=m, A_6=a_1, A_7=a_2 \end{aligned} \tag{8}$$

Esq.(12) is changed as follow

$$y = A_0+A_1X_1+A_2X_2+A_3X_3+A_4X_4+A_5X_5+A_6X_6+A_7X_7 \tag{9}$$

Table 3 shows the common statistic values. The correlation coefficient R = 0.974, determination coefficient $\overline{R}^2$ = 0.949, the adjustment determination coefficient $\overline{R}^2$ = 0.931, the Std. Error of the Estimate S =0.0670. As the equation has a number of explained variables, the determination should be based on the adjustment determination coefficient $\overline{R}^2$. As can be seen from the output that $\overline{R}^2$ is close to 1, the fit degree is high. So the representativeness of proposed constitutive model is strong.

Model	R	R Square	Adjusted R Square	Error of the Estimate
1	0.974(a)	0.949	0.931	0.0671449560

a Predictors:(Constant), x_7,x_6,x_4,x_2,x_3,x_5,x_1 b Dependent Variable:y

Table 3. Model Summary

The analysis is listed in Table 4. The significant test of regression equation is based on the table. Total in Sum of Squares is 835.005, Regression in Sum of Squares and Regression in

Mean Square are 413.512 and 59.073 respectively. Residual in Sum of Squares and Residual in Mean Square are 421.492 and 0.451 respectively. The test statistic observations F = 130.902. The concomitant probability p is approximately 0. The linear relationship between variables x and y is significant, which create a linear model.

Model		Sum of Squares	df	Mean Square	F	Sig.
1	Regression	413.512	7	59.073	130.902	0.000(a)
	Residual	421.492	934	0.451		
	Total	835.005	941			

a Predictors: (Constant),x_7,x_6,x_4,x_2,x_3,x_5,x_1 b Dependent Variable:y

Table 4. ANOVA (b)

Table 5 shows the regression coefficient analysis. As can be seen from the table and the estimated value of the test results, the corresponding variable regression coefficient A0=-8.27366, A1=50.158,A2=-296.555,A3 =14253.359,A4 =-0.053,A5=0.242,A6 =2.316,A7 =-0.505. The concomitant probability p is 0, whose regression is a significant. From comparison of regression coefficients, those indicate that the constitutive model has a significant meaning. The sensitivity coefficient m A5=0.242 of strain rate resulted from regression is good close to the replaced m value.

Model		Unstandardized Coefficients		Standardized Coefficients	t	Sig.
		B	Std. Error	Beta		
1	(Constant)	-8.27366	1.818		-9.728	0.000
	X_1	50.158	7.917	1.303	6.335	0.000
	X_2	-296.555	53.608	-0.934	-5.532	0.000
	X_3	14253.359	1402.791	0.342	10.161	0.000
	X_4	-0.053	0.012	-0.108	-4.601	0.000
	X_5	0.242	0.045	0.474	5.382	0.000
	X_6	2.316	0.553	0.143	4.186	0.000
	X_7	-0.505	0.463	-0.135	-1.091	0.000

a Dependent Variable：y

Table 5. Coefficients (a)

The analysis of the regression equation is a meaningful, and the following relation is got.

$$y = -8.27366 + 50.158X_1 - 296.555X_2 + 14253.359X_3 - 0.053X_4 + 0.242X_5 + 2.316X_6 - 0.505X_7 \quad (10)$$

From the inverse transform of equations (9) and (10), equation (6) becomes:

$$\begin{aligned} \sigma &= \exp(\text{-}8.27366+50.158 f_p\text{-}296.555 f_p{}^2 + 14253.359 / T) \cdot \varepsilon^{\text{-}0.053} \cdot \\ &\cdot \dot{\varepsilon}^{0.242} \cdot [1-\beta f_L]^{2.316} \cdot [1+(2.1\times 10^4 \dot{\varepsilon})^{0.242} f_p]^{\text{-}0.505} \end{aligned} \quad (11)$$

Equation (11) is a constitutive relationship of thixotropic plastic forming of SiCp/AZ61 composites.

Fig.18 is the real stress test - a true strain curves and regression curve of the results of the comparison, Solid line is the experimental curve, dotted line is the calculation of one. The results calculated by multiple non-linear regression method are good agreement with experimental ones. So the proposed constitutive model has the higher forecast precision and practical significance.

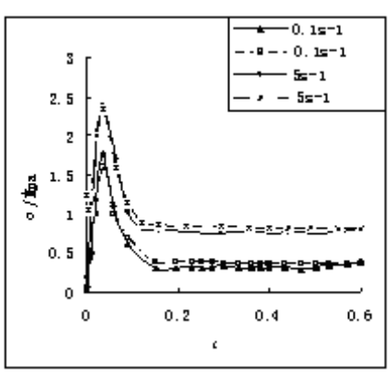

(a) 3vol.% SiC_P/AZ61,570℃

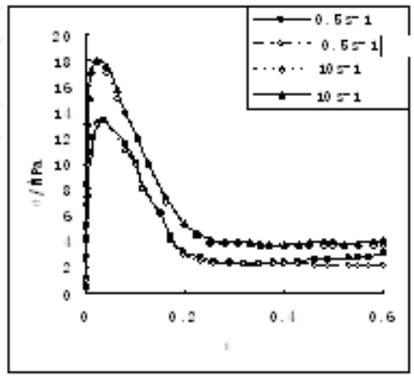

(b) 6vol.% SiC_P/AZ61,560℃

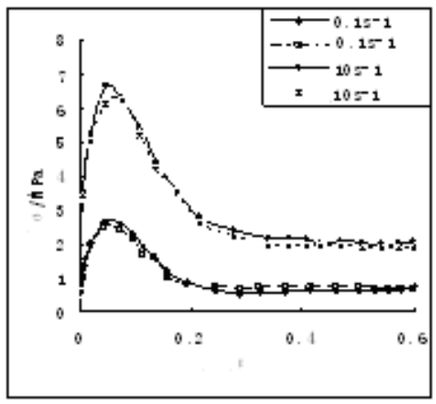

(c) 9vol.% SiC_P/AZ61,530℃

Fig. 18. A comparison between true strain—stress curves of the test and regression curves

6. Numerical simulation for thixotropic plastic forming of composites

To investigate thixoforming process with numerical simulation method, which is a nonlinear system, some assumptions are taken as follow: (1) The semi-solid material is assumed as a continuous and incompressible one. (2) The solid grains in semi-solid metal are uniformly distributed in liquid phase, and because of the large deformation in forming, the semi-solid material is considered as an isotropy uniform medium. According to the above assumptions, the material deformation in thixoforming is supposed as a rigid viscoplastic one.

The material adopted in this paper was SiCp/AZ61 composite, and the simulations were performed in thixo-forging and forging. The flow stress model of SiCp/AZ61 composite in thixo-forging is expressed as follow [Yan &Wang, 2011].

$$\sigma = \exp(-8.27366 + 50.158 f_p - 296.55 f_p^{\,2} + 14253.359 / T)$$

$$\cdot \varepsilon \text{ -0.053} \cdot \dot{\varepsilon} \text{ 0.242} \cdot \left(1 - \beta f_L\right) \text{2.316} \cdot [1 + (2.1 \times 10^4 \dot{\varepsilon}) \text{ 0.242 } f_p] \text{-0.505} \qquad (12)$$

where σ is the stress; ε the strain; z $\dot{\varepsilon}$ the strain rate; T temperature; β constant(β=1.5); f_p is Volume fraction of SiC particle; f_L is liquid volume fraction

For establishing material modal of SiCp/AZ61 composite in forging, true stress-strain curves at various temperature and strain rates were performed by mean of isothermal compression experiments.

In this study, the workpiece is formed by the close-forge method. The experiment set-up was shown in Fig.19. Fig.20 shows the workpiece, whose structure and flow character are complicated. Comparisons between forging and thixo-forging of the workpiece will be done and predicted in advance using numerical simulation. This is an effective method to instruct application of semi-solid forming technology into its practice production.

The same simulated parameters are used to analyze the differences of mechanics properties and flow rule between forging and thixo-forging processes. The materials are normal and semi-solid SiCp/AZ61 composite respectively. Environment temperature is 20℃, warm-up temperature of the die is 320℃. The friction model is constant shearing stress model, whose coefficient is 0.25. Billet size is ø50×18.5mm, which is meshed to 50000 tetrahedron elements. Stroke of up-die is 14mm.

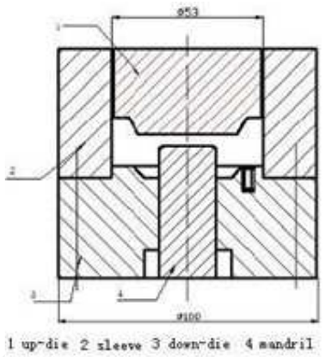

Fig. 19. Experiment set-up

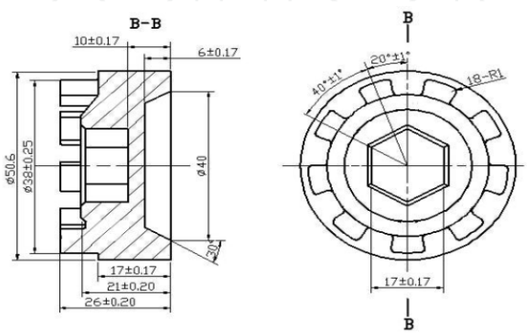

Fig. 20. SiCp/AZ61 composite workpiece

Fig.21 and Fig.22 give the filling stages simulated results in forging and thixo-forging processes respectively. Compared with the two kind of forming processes, it can be concluded that both had the basically identical deformation processes. In the initial stage, the hexagon hole in central section of workpiece was extruded and the rest moved in the rigid motion shown in Fig.21a, Fig.22a. As the stroke increased, metal deformation entered into the second stage, in which metal flowed from central to around in the extrusion pressure, and the cetral protruded and bottom platforms were formed (Seen Fig.21b, Fig.22b). In the last stage, the metal could be filled up claw easily in thixo-forging process, and could not be filled up claw in forging process (Seen Fig.21c, Fig.22c). Therefore, forging was more difficult in filling cavity than thixo-forging.

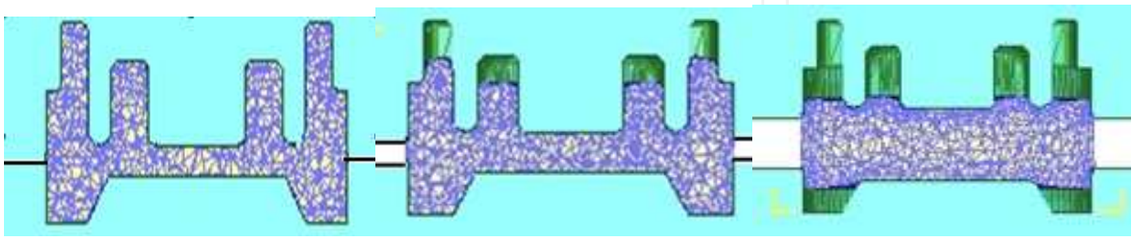

Fig. 21. Filling stages simulated results in thixo-forging process

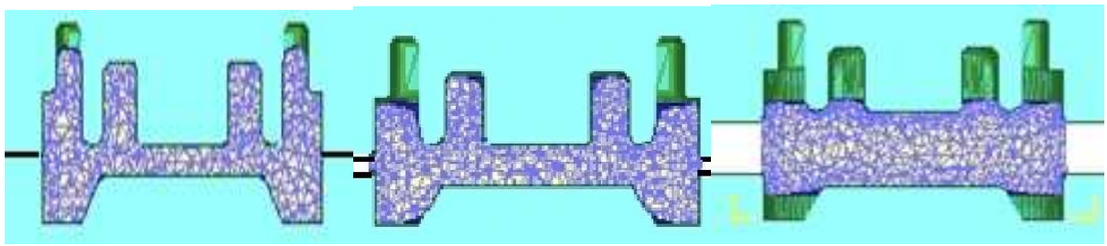

Fig. 22. Filling stages simulated results in forging process

Fig. 23. shows the effective stress distributions at different temperatures in thixo-forging process. The effective stress distribution was more uniform and its value was smaller with the increasing of forming temperature, which was contributed from the excellent fluidity of semi-solid composite.

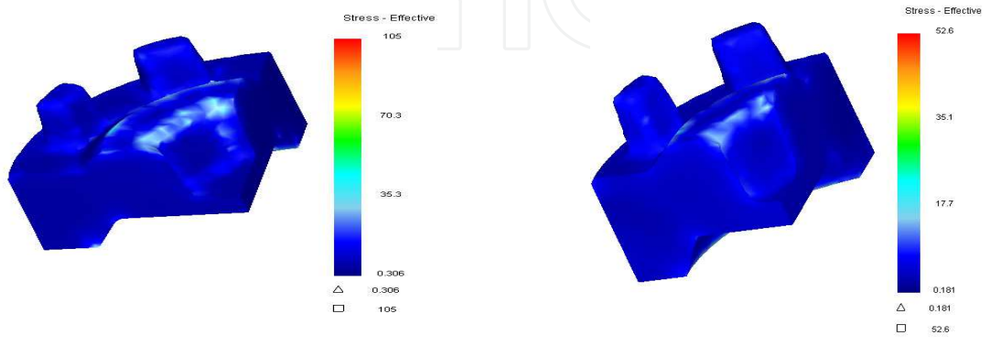

(a) 530℃ (b) 560℃

Fig. 23. Effective stress distributions at different temperatures in thixo-forging process

Fig. 24. shows the effective stress distributions at different volume fraction of SiC particle in thixo-forging process. The effective stress was increased with the increasing of volume fraction of SiC particle.

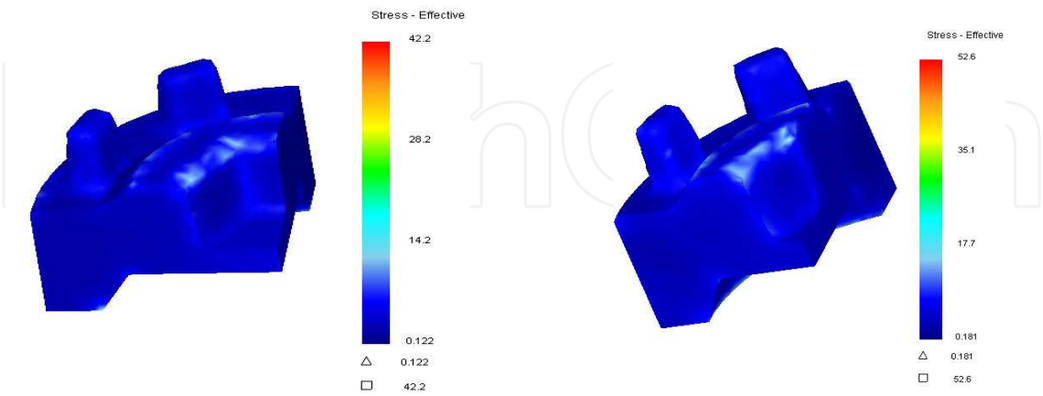

(a) Vol.3% SiC_P/AZ61, 560℃ (b) Vol.6% SiC_P/AZ61, 560℃

Fig. 24. Effective stress distributions at different volume fraction of SiC particle in thixo-forging process

Fig. 25 shows temperature distributions at different volume fraction of SiC particle in thixo-forging process. When the volume fraction of SiC particle was 3%, the fluctuation period of temperature was 558～561℃, whose changed value was small. When the volume fraction of SiC particle was 6%, the fluctuation period of temperature was 558～572℃, whose changed value was more greater than that of the former. It could be gained that the temperature distribution in the latter was worse than that in the former.

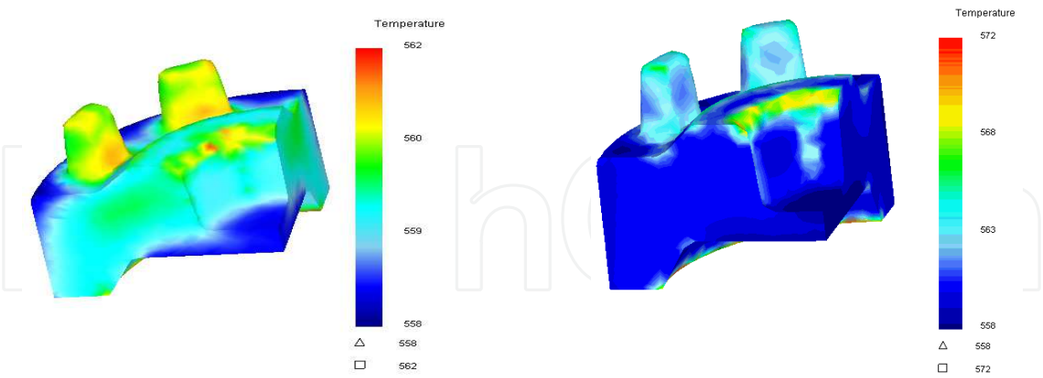

(a) Vol.3% SiC_P/AZ61, 560℃ (b) Vol.6% SiC_P/AZ61, 560℃

Fig. 25. Temperature distributions at different volume fraction of SiC particle in thixo-forging process

Fig.26 shows the traditional forging and thixo-forging workpieces of SiCp/AZ61 composite. The thixo-forging has better fill effect and surface finish quality of workpiece than the traditional forging, which could achieve near-end deforming with high quality of workpiece in the former. Those coincide with the simulation results, which indicate that semi-solid

SiCp/AZ61 composite has good flow property, and can be used to form complicated workpiece.

(a) Traditional forging workpiece (b) Thixo-forging workpiece

Fig. 26. Traditional forging and thixo-forging workpieces of composite

7. Conclusions

The microstructural structures of magnesium matrix composite were studied in three different casting processes. The results indicated that SiCp/AZ61 composites fabricated in stirring melt casting process, compared to those in fully liquid stirring casting process and in semi-solid stirring casting process, possessed fairly uniform distribution of SiC particulates and few porosity rate. It was an ideal metal matrix composites fabricated process.

Under the experimental conditions, the optimum processing plan of SiCp/AZ61 composites fabricated by a stirring melt casting method were the volume fraction of SiC particles 6%, stirring temperature 595℃ and stirring time 5 min. In addition, the effects of volume fraction of SiC particles on the mechanical properties of SiCp/AZ61 composites was the most important among three factors (volume fraction of SiC particles, stirring temperature and stirring time), the second were stirring time and stirring temperature.

Semi-solid isothermal heat treatment technology was used for the partial remelting of SiCp/AZ61 composites. A fine semi-solid microstructure was obtained, whose equal-area diameter size was between 60μm and 85μm, and the effective liquid volume fraction was about 31%～38%. The optimal technological parameters of SiCp/AZ61 composites were the reheating temperature of 595℃～600℃ and an isothermal holding time of 30min～60min.

Compression tests on semi-solid SiCp/AZ61 magnesium matrix composites were carried out. Influences of strain-rate, strain, temperature and volume fraction of SiC particles on flow stress were analyzed. The results show that the flow stress of semi-solid SiCp/AZ61 composites is sensitive to temperature and strain rate. Meanwhile the flow stress increases with the increasing of the volume fraction of SiC particles.

The influence of deformation temperature, strain rate, strain, liquid volume fraction, volume fraction of reinforcement on flow stress in composites thixotropic plastic deformation process was considered. A new constitutive model of composites in thixotropic plastic

deformation process was proposed. The constitutive equation of SiCp/AZ61 composites was obtained with the multiple nonlinear regression method based on data of thixotropic compression test. The calculated results were good agreement with the experimental ones. It is used to guide composites thixotropic plastic deformation process.

Numerical simulation can provide a help for the analysis of thixoforging process, and behavior of metal flow has been obtained. The effective stress distribution was more uniform and its value was more smaller with the increasing of forming temperature. The effective stress was increased with the increasing of volume fraction of SiC particle. The temperature distrubition was worse with the increasing of volume fraction of SiC particle. The differences between traditional forging and thixo-forging processes were analyzed. Results indicated that thixo-forging was better in filling cavity than forging. So the complicated workpiece can be done once in thixo-forging. Numerical simulation results are accorded with experimantal ones.

8. Acknowledgement

This research was supported jointly by grant # 50465003, # 50765005 and # 51165032 from the National Natural Science Foundation of China, Innovative Group of Science and Technology of College of Jiangxi Province and the Jiangxi Province Education Commission Foundation.

9. References

Hai, Z. Y., Xing, Y. L. (2004). Review of recent studies in magnesium matrix composites. *Journal of Materials Science*, Vol. 39: 6153-6171

Zhou, W., Xu, Z. M. (1997). Casting of SiC reinforced metal matrix composites. *Journal of Materials Processing Technology*, Vol. 63 , No.3: 358-363

Kang, C. G., Choi, J. S., Kim, K. H. (1999). The effect of strain rate on macroscopic behavior in the compression forming of semi-solid aluminum alloy. *Materials Processing Technology*, Vol.88, No.1-3: 159-168

Zhang, X. Q., Wang, H. W., Liao, L. H. (2004). In situ synthesis method and damping characterization of magnesium matrix composites. *Composites Science and Technology*, Vol. 67:720-727

Mordike, B. L. (2002). Development of highly creep resistant magnesium alloys. *Journal of Materials Processing Technology*, Vol. 117, No.3: 391-394

Flemings, M. C. (1991). Behavior of metal alloy in the semi-solid state. *Metall Trans A*, Vol.22, No.5: 957-981

Yan, H., Xia, J. C. (2005). Theoretical analysis of plastic forming process for semi-solid material. *Materials Science Forum*, Vol.488-489, 389-392

Yan, H., Zhang, F. Y. (2005). Structure evolution of AZ61 magnesium alloy in SIMA process. *Transactions of Nonferrous Metals Society of China*, Vol.15, No.3, 560-564

Yan, H., Zhang, F. Y. (2006). Microstructural evolution of semi-solid AZ61 magnesium alloy during reheating process. *Solid State Phenomena*, Vol.116-117, 275-278

Yan, H., Zhou, B. F. (2006). Thixotrpic deformation behavior of semi-solid AZ61 magnesium alloy during compression process, *Materials Science and Engineering B*, Vol.132, No.1-2, 179-182

Yan, H., Zhou, B. F. (2006). Constitutive model of thixotropic plastic forming for semi-solid AZ61 magnesium alloy. *Solid State Phenomena*, Vol.116-117, 577-682

Yan, H., Zhou, B. F. (2008). Study on thixo-forging of AZ61 wrought magnesium alloy. *Solid State Phenomena*, Vol.141-143, 577-682

Yan, H., Fu, M.F., Zhang, F. Y., Chen, G. X. (2007). Research on properties of SICp/AZ61 magnesium matrix composites in fabrication processes. *Materials Science Forum*, Vols. 561-565: 945-948

Yan, H., Lin, L. S. B., Pan, W. (2008). Study of SICp/AZ61 composites. *Solid State Phenomena*, Vols. 141-143 :551-555

Yan, H., Zhang, F. Y., Pan, W. (2008). Microstructural evolution of SiCp/AZ61 composites during partial remelting. *Solid State Phenomena*, Vols. 141-143 :545-549

Zhang, F. Y., Ye, J. X., Yan, H. (2011). Effects of SiC particle and holding time on semi-solid microstructure of SICp/AZ61 composites. *Advanced Materials Research*, Vols. 152-153: 628-633

Yan, H., Wang, J. J. (2011). Thixotropic compression deformation behavior of SICp/AZ61 magnesium matrix composites. *Transations of Nonferrous Metals Society of China*, Vols. 20: s811-s814

Yan, H., Wang, J. J.,Zhang, F. Y. (2011). A constitutive model for thixotropic plastic forming of semi-solid composites. *Advanced Materials Research,* Vols. 154-155:690-693

Yan, H., Huang, W. X. (2011). Numerical simulation on thixo-forging of magnesium matrix composite. *Advanced Materials Research,* Vols. 189-193:2535-2538

Bao, G., Lin, Z.(1996). High strain rate deformation in particle reinforced metal matrix composites. *Acta Materialia*, Vol.44, No. 3: 1011-1019.

Li, Y., Ramesh, K.T., Chin, E.S.C.(2000). The compressive viscoplastic response of an A359/SiCp metal—matrix composite and of the A359 aluminum alloy matrix. *International Journal of Solids and Structures*, Vol. 37, No. 51:7547-7562.

Yan, H., Huang, X. ,Hu, Q. (2010). Damping capacity of SICp/AZ61 composites. *Advanced Materials Research*, Vols. 123-125 : 35-38

Yan, H., Huang, Z. M. (2011). Study on creep properties of SiCp/AZ61 composites. *Advanced Materials Research*, Vols. 189-193: 4227-4230

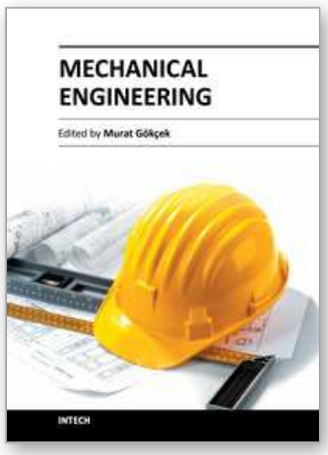

Mechanical Engineering

Edited by Dr. Murat Gokcek

ISBN 978-953-51-0505-3
Hard cover, 670 pages
Publisher InTech
Published online 11, April, 2012
Published in print edition April, 2012

The book substantially offers the latest progresses about the important topics of the "Mechanical Engineering" to readers. It includes twenty-eight excellent studies prepared using state-of-art methodologies by professional researchers from different countries. The sections in the book comprise of the following titles: power transmission system, manufacturing processes and system analysis, thermo-fluid systems, simulations and computer applications, and new approaches in mechanical engineering education and organization systems.

How to reference

In order to correctly reference this scholarly work, feel free to copy and paste the following:

Hong Yan (2012). Study on Thixotropic Plastic Forming of Magnesium Matrix Composites, Mechanical Engineering, Dr. Murat Gokcek (Ed.), ISBN: 978-953-51-0505-3, InTech, Available from: http://www.intechopen.com/books/mechanical-engineering/study-on-thixotropic-plastic-forming-of-magnesium-matrix-composites

INTECH
open science | open minds

InTech Europe
University Campus STeP Ri
Slavka Krautzeka 83/A
51000 Rijeka, Croatia
Phone: +385 (51) 770 447
Fax: +385 (51) 686 166
www.intechopen.com

InTech China
Unit 405, Office Block, Hotel Equatorial Shanghai
No.65, Yan An Road (West), Shanghai, 200040, China
中国上海市延安西路65号上海国际贵都大饭店办公楼405单元
Phone: +86-21-62489820
Fax: +86-21-62489821

© 2012 The Author(s). Licensee IntechOpen. This is an open access article distributed under the terms of the Creative Commons Attribution 3.0 License, which permits unrestricted use, distribution, and reproduction in any medium, provided the original work is properly cited.

IntechOpen

IntechOpen